



Protostars in time and space: results from the Herschel Orion protostar survey

S. T. Megeath

Ritter Astrophysical Research Center, Dept. of Physics & Astronomy, University of Toledo,
Toledo OH, 43606, USA, e-mail: s.megeath@utoledo.edu

Abstract. The Herschel Orion Protostar Survey studied 330 protostars in the Orion molecular clouds with *Spitzer*, *Herschel*, *Hubble* and ground based telescopes, obtaining spectral energy distributions and far-IR spectra. We review recent results from this survey on the evolution of infall, the connection between outflow and accretion, and the clearing of protostellar envelopes by outflows. We then discuss kinematical studies of infall and outflow using ALMA and SOFIA, and the prospects for constraining the birthline of protostars.

Key words. Stars: formation – Stars: protostars – ISM: jets and outflows – Infrared: stars – Submillimeter: stars

1. Introduction

The conversion of interstellar gas into stars can be directly observed in protostars: growing stellar objects embedded within collapsing envelopes of gas and dust. Detailed studies of protostars in time and space, i.e. their evolution and their dependence on birth environment, are now possible due to a remarkable decade of wide-field, space-based IR astronomy (e.g. Dunham et al. 2014). Surveys with *Spitzer*, *Herschel*, *WISE* and ground-based sub-mm telescopes, have identified and characterized over a thousand protostars in nearby (< 1 kpc) molecular clouds, providing a rich sample for studies of protostellar evolution (e.g. Kryukova et al. 2012; Dunham et al. 2013; Fischer et al. 2016; Megeath et al. 2016).

The Herschel Orion Protostar Survey (hereafter: HOPS) assembled 1.2-870 μm SEDs of 330 protostars in the Orion A and B molecular clouds from 2MASS photometry at 1-2.5 μm , *Spitzer* photometry and spec-

troscopy from 3.6 to 35 μm , *Herschel* photometry at 70, 100 and 160 μm , and ground-based 350 and 870 μm data (Furlan et al. 2016). These include deeply embedded protostars first identified by *Herschel* (Stutz et al. 2013; Tobin et al. 2015). The SEDs are complemented by HST imaging of 283 protostars (Kounkel et al. 2016; Booker et al. submitted). PACS 57-196 μm spectra were obtained for 52 protostars (Manoj et al. 2013, 2016; Tobin et al. 2016). These data products are being distributed to the community through ESA and NASA's InfraRed Science Archive (IRSA).

2. The evolution of infall & outflow

The shapes of protostellar SEDs evolve as the densities of the envelopes and the rates of mass infall decrease (Fig. 1, see discussion of caveats in Furlan et al. 2016). Using the HOPS SEDs, Fischer et al. (2017) find a systematic decrease in the bolometric lumi-

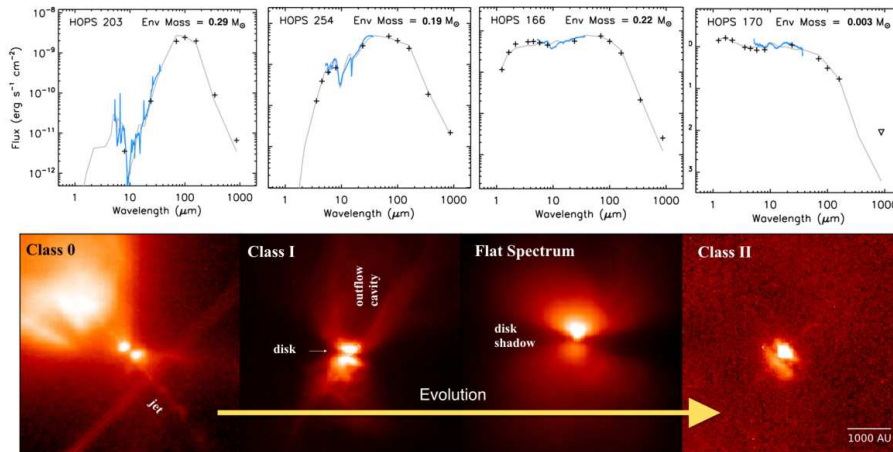


Fig. 1. Top: SEDs of Orion protostars assembled with the data from HOPS for (left to right) a Class 0 protostar, a Class I protostar, a flat spectrum protostar, and a Class II object (a pre-main sequence star with disk, Furlan et al. 2016). The + show fluxes from photometry, blue lines show fluxes from IRS spectra, and the black lines are models. **Bottom:** protostars in the Orion clouds imaged by HST/WFC3 in scattered light at $1.6 \mu\text{m}$. Light from the central protostars are scattered by dust grains in the envelopes, the walls of outflow cavities, and in disks (Booker et al. submitted). Note the SEDs are primarily for intermediate inclination angles (which are more common) while the images are selected to have a close to edge-on orientation.

nosities of protostars between the Class 0 and Class I phases. Furthermore, using radiative transfer model fits to the SEDs (Furlan et al. 2016), they argue that the masses of the inner ($< 2500 \text{ AU}$) envelopes are decreasing exponentially with time. The accompanying decreases in mass infall rates and accretion rates can then explain the decline in the luminosities of the protostars. By requiring a range of

final stellar masses for the growing protostars, they also reproduce the observed, broad spread of luminosities using simple models. Episodic accretion also contributes to this spread; with outbursts being detected towards two of the 330 Orion protostars between 2004 and 2010 (Fischer et al. 2012; Safron et al. 2013).

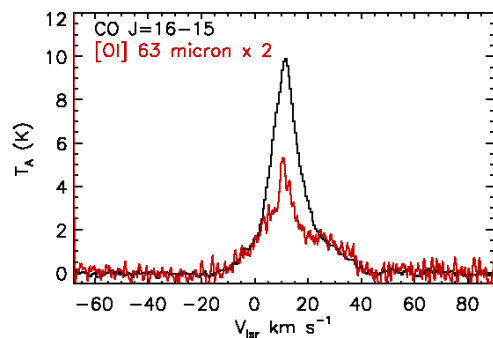


Fig. 2. Terahertz CO (16-15) and [OI] spectra of the OMC2 FIR3 (i.e. HOPS 370) outflow obtained with GREAT on SOFIA. (Megeath et al. in prep.)

Far-IR rotational lines of CO are commonly detected in PACS spectroscopy of the protostars. Manoj et al. (2013, 2016) find that the total luminosity in the far-IR lines is correlated with bolometric luminosity, but there is no strong dependence with evolutionary class. This result establishes a relationship between the mechanical luminosity of outflows and the radiant luminosity generated by mass accretion. Using outflow cavities detected in scattered light with HST $1.6 \mu\text{m}$ imaging (Fig. 1), Booker et al. (submitted) measure the fraction of each envelope cleared by outflows to create the observed cavities. They find no evidence for a progressive growth in the cavities and identify evolved protostars with narrow outflow cavities. They conclude that the clearing of cavities by outflows cannot account

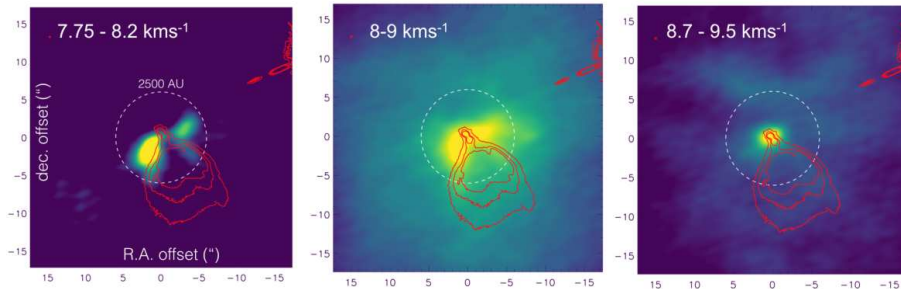


Fig. 3. ALMA 12-meter, ACA and total power C^{18}O (2-1) observations of the edge-on protostar HOPS 171 (reduced by Z. Nagy). The contours show the scattered light emission of the protostar from HST. The panels show (left) gas tracing the edges of the outflow cavity in the blue-shifted gas, (middle) the irregular morphology of the envelope at the systemic velocity, and (right) infalling gas in the red-shifted gas.

for the termination of mass infall or the low ($\sim 40\%$) star formation efficiency of cores.

3. The kinematics of infall & outflow

SOFIA and ALMA are now being used to probe the kinematics of infall and outflow. SOFIA/GREAT observations have resolved far-IR lines in the powerful OMC2 FIR3 outflow, which extends over 0.1 pc in far-IR lines and exhibits non-thermal radio emission (Gonzales et al. 2016; Osorio et al. 2017). The lineshape at the end of the outflow suggests that the far-IR line emission originates in the terminal bow-shock at this position (Fig. 2).

ALMA observations of the colder gas map the motions and structures in inner envelopes (< 2500 AU), as shown in Fig. 3. These data demonstrate the ability of ALMA to detect the infall and rotation of gas accelerated by the gravity of the central protostar. They show that the axial symmetry adopted in rotating collapse models are not present in the observed protostar (e.g. Terebey, Shu, & Cassen 1984).

4. Toward a stellar birthline

One of the next goals for HOPS is to measure the birthline, the loci of masses and radii at the onset of pre-main sequence contraction (Palla & Stahler 1990). ALMA can observe the rotation of protostellar disks and measure the masses of the central protostars. High dispersion, near-IR spectrometers such as IGRINS and iSHELL can detect veiled photospheric features and determine T_{eff} which, in combination with the measured luminosities of the

protostars, can be used to calculate their radii. Such observations promise a test of models of the birthline and its contribution to the apparent age spreads of pre-main sequence stars found by Palla & Stahler (2000).

Acknowledgements. This work is that of the HOPS team and supported by awards provided by NASA.

References

- Booker, J. J., et al. submitted
- Fischer, W. J., et al. 2012, *ApJ*, 756, 99
- Fischer, W. J., et al. 2016, *ApJ*, 827, 96
- Fischer, W. J., et al. 2017, *ApJ*, 840, 17
- Furlan, E. et al. 2016, *ApJ*, 224, 45
- Dunham, M. M., et al. 2013, *AJ*, 145, 19
- Dunham, M. M., et al. 2014, in *Protostars and Planets VI*, H. Beuther et al. eds (Univ. Arizona Press, Tucson), 195
- González-García, B., et al. 2016, *A&A*, 596, 26
- Kounkel, M., et al. 2016, *ApJ*, 821, 52
- Kryukova, E., et al. 2012, *AJ*, 144, 31
- Manoj, P., et al. 2013, *ApJ*, 763, 83
- Manoj, P., et al. 2016, *ApJ*, 831, 69
- Megeath, S. T., et al. 2016, *AJ*, 151, 5
- Osorio, M., et al. 2017, *ApJ*, 840, 36
- Palla, F. & Stahler, S. W. 1990, *ApJ*, 360, L47
- Palla, F. & Stahler, S. W. 2000, *ApJ*, 540, 255
- Safron, E. J., et al. 2015, *ApJ*, 800, L5
- Stutz, A. M., et al. 2013, *ApJ*, 767, 36
- Terebey, S., Shu, F. H. & Cassen, P. 1984, *ApJ*, 286, 529
- Tobin, J. J., et al. 2015, *ApJ*, 798, 128
- Tobin, J. J., et al. 2016, *ApJ*, 831, 36